

Structure Enabled Design of BAZ2-ICR, A Chemical Probe Targeting the Bromodomains of BAZ2A and BAZ2B

Ludovic Drouin,[†] Sally McGrath,[†] Lewis R. Vidler,[†] Apirat Chaikwad,[‡] Octovia Monteiro,^{‡,§} Cynthia Tallant,^{‡,§} Martin Philpott,^{‡,§} Catherine Rogers,^{‡,§} Oleg Fedorov,^{‡,§} Manjuan Liu,[†] Wasim Akhtar,[†] Angela Hayes,[†] Florence Raynaud,[†] Susanne Müller,^{‡,§} Stefan Knapp,^{*,‡,§} and Swen Hoelder^{*,†}

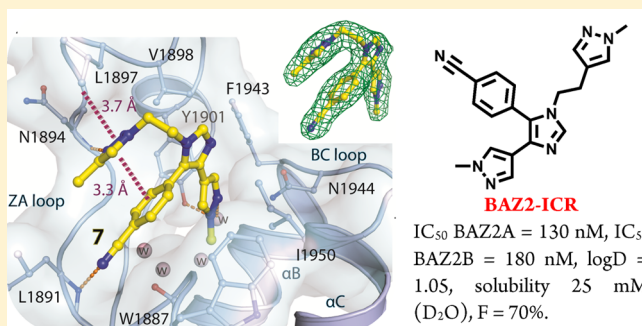
[†]The Institute of Cancer Research, Division of Cancer Therapeutics, Cancer Research UK Cancer Therapeutics Unit, 15 Cotswold Road, Sutton, London SM2 5NG, U.K.

[‡]The Structural Genomic Consortium, University of Oxford, Old Road Campus Research Building, Roosevelt Drive, Headington, Oxford OX3 7DQ, U.K.

[§]Target Discovery Institute, University of Oxford, NDM Research Building, Roosevelt Drive, Headington, Oxford OX3 7FZ, U.K.

S Supporting Information

ABSTRACT: The bromodomain containing proteins BAZ2A/B play essential roles in chromatin remodeling and regulation of noncoding RNAs. We present the structure based discovery of a potent, selective, and cell active inhibitor **13** (BAZ2-ICR) of the BAZ2A/B bromodomains through rapid optimization of a weakly potent starting point. A key feature of the presented inhibitors is an intramolecular aromatic stacking interaction that efficiently occupies the shallow bromodomain pockets. **13** represents an excellent chemical probe for functional studies of the BAZ2 bromodomains in vitro and in vivo.



■ INTRODUCTION

Bromodomains are acetyl-lysine specific epigenetic reader domains and an emerging new target class for the design of protein interaction inhibitors that selectively modulate gene transcription.^{1,2} However, the discovery of potent and selective inhibitors has been mainly focused on the bromo and extra-terminal (BET) subfamily of bromodomains (BRD2, BRD3, BRD4, BRDT) for which first inhibitors have reached clinical testing¹ and no potent and selective inhibitors are known for the large majority of bromodomains.³ This paucity of selective chemical probes represents a barrier for the identification and validation of additional bromodomains as therapeutic targets. Chemical probes have several advantages for target identification and validation over commonly used genetic techniques like RNAi experiments and dominant negative mutants.⁴ This is particularly relevant for bromodomains because these proteins often function as scaffolding proteins in larger multidomain proteins, suggesting that depletion of the entire protein, e.g., by RNAi does not reflect inhibition of a specific interaction by a small molecule drug.

Two homologous bromodomains for which no potent and selective inhibitors have been published so far are BAZ2A and BAZ2B. Bromodomain adjacent to zinc finger domain (BAZ) represents a family of ubiquitously expressed proteins (BAZ1A, BAZ1B, BAZ2A, and BAZ2B) with a similar domain structure.⁵ BAZ2A forms with ATPase sucrose nonfermenting-2 homo-

logue (SNF2h) the nucleolar remodeling complex (NoRC), a member of the imitation switch chromatin remodeling complexes (ISWI).⁶ NoRC has been shown to regulate expression of noncoding RNAs and also establishes a repressive heterochromatic structure at centromeres and telomeres.⁷ Interestingly, mutations in the BAZ2A bromodomain that abolish histone binding impair association of NoRC with chromatin and transcriptional repression.⁸ In addition, single nucleotide polymorphisms (SNPs) in the BAZ2B gene locus have been identified as being associated with sudden cardiac death⁹ and high expression levels of BAZ2B have found to be associated with poor outcome of pediatric B cell acute lymphoblastic leukemia (B-ALL), raising the potential that BAZ2B inhibitors may have therapeutic potential for this cancer. Furthermore, a recent publication reports that BAZ2A is involved in maintaining prostate cancer cell growth and establishes a correlation between BAZ2A expression and recurrence in prostate cancer.¹⁰

Interestingly, BAZ2A/B show low predicted druggability¹¹ due to an open binding site that lacks the deep and enclosed pocket characteristic for the BET subfamily bromodomains. No potent and selective inhibitors have been published, although a number of weak and nonselective fragments have been reported

Received: December 19, 2014

Published: February 26, 2015

recently.¹² To identify chemical starting points for these challenging targets, we screened a series of putative BRD inhibitors obtained in the course of a virtual screening campaign.¹³ Consistent with the difficult nature of this target, we identified a single compound (**1**, Figure 1) as a weak

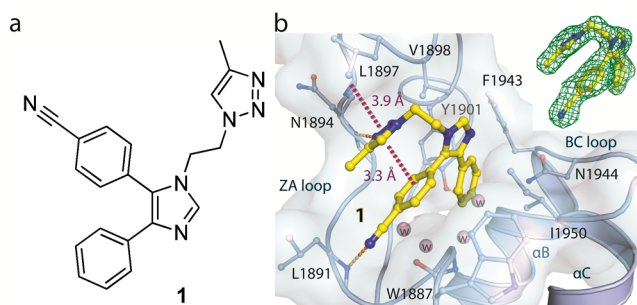


Figure 1. Interaction between BAZ2B and **1**. (a) Chemical structure of **1**. (b) 1.8 Å cocrystal structures of **1** bound to BAZ2B (PDB: 4XUA). Main interacting residues are shown in ball and stick representation and are labeled. Conserved water molecules (w) in the KAc binding site are shown as pink spheres. The inset shows the $|2F_{\text{O}}| - |F_{\text{C}}|$ omitted map for **1**, contoured at 1σ .

inhibitor of BAZ2A ($\text{IC}_{50} = 51 \mu\text{M}$) and BAZ2B ($\text{IC}_{50} = 26 \mu\text{M}$). Here we describe the optimization of **1**, ultimately resulting in the discovery of **13** (BAZ2-ICR), a potent and selective chemical probe of the BAZ2 bromodomains.

RESULTS AND DISCUSSION

To shed light on the binding mode and derive design hypotheses for the optimization of **1**, we solved the crystal structure of **1** bound to BAZ2B to 1.8 Å resolution. This cocrystal structure revealed a number of interesting features.

Bromodomains bind to acetylated lysines (KAc) through a conserved pocket (KAc pocket). All bromodomain inhibitors known to date bind to this pocket through a KAc mimetic group, often a heterocyclic ring that engages in hydrogen bonds with a conserved asparagine residue and a conserved water molecule.¹⁴ We initially hypothesized that the methyl-triazolo group of **1** (a putative KAc mimetic) acts as the KAc mimetic. Surprisingly, the cocrystal structure revealed the hydrophobic phenyl ring of **1** occupied the KAc binding pocket despite the presence of conserved water molecules and the asparagine residue (N1944, numbering according to isoform 4 (gil 7304923)), both of which typically act as hydrogen bond donors (Figure 1).

Another surprising feature of the structure of **1** bound to BAZ2B was an intramolecular, face-to-face π -stacking interaction formed by the nitrile substituted phenyl ring and the triazole ring of **1**. The distance between these two rings of $\sim 3 \text{ \AA}$ is in the typical range for face-to-face π -stackings. The energetics of a π -stacked conformation is typically driven by two factors: solvent exclusion and electronic complementarity of the two aromatic rings to minimize the repulsion of the π -clouds.¹⁵ We performed a field analysis using the XED force field from Cresset¹⁶ to investigate the electronic characters of the two aromatic rings which form the stacking interaction. This analysis showed that the triazole ring was electron rich on the face of the ring and the nitrile substituted phenyl ring electron poor (see Supporting Information (SI)). These complementary properties thus likely contributed to the formation of the stacking conformation.

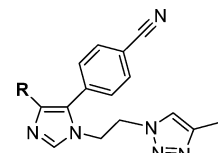
Furthermore, the nitrile function and one of the triazole ring nitrogen atoms engage in hydrogen bonds with backbone atoms Leu1891 and Asn1894 (Figure 1b). The internal π -stacking arrangement of these two aromatic groups thus represented an excellent shape and hydrogen bonding complementary to the open BAZ2B pocket, maximizing polar and hydrophobic interactions, and was thus likely critical for the observed potency and selectivity.

Our aim starting from **1** was to identify a potent and selective inhibitor of BAZ2A/B that is active in the cellular context in the low/submicromolar range. We therefore aimed to improve the in vitro activity 100–200-fold while maintaining high selectivity for BAZ2A/B.

On the basis of the crystal structure, we hypothesized that a large gain in potency can be achieved by replacing the phenyl ring of **1** that occupied the KAc pocket by a moiety that mimics the hydrogen bond network of KAc. We thus designed a small set of compounds in which the phenyl group of **1** was replaced by known KAc mimetics¹ or other heterocycles that can engage in hydrogen bonds (Table 1) and set out to develop a concise and efficient synthetic route to these compounds.

Careful optimization led to the three-step route depicted in Scheme 1. An initial three component Van Leusen imidazole formation enabled us to access imidazole intermediates in 10–

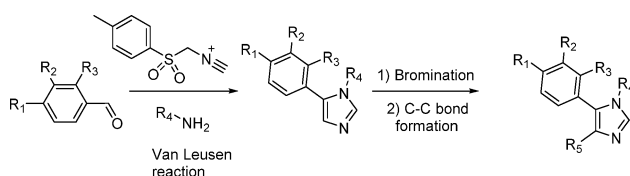
Table 1. Structure–Activity Relationship of Triazole Substituted Compounds^a



Compound	R	BAZ2A IC_{50} (LE)	BAZ2B IC_{50} (LE)
1		51 (0.22)	26 (0.23)
2		4.0 (0.27)	4.4 (0.27)
3		>50 (<0.22)	>50 (<0.22)
4		7.8 (0.27)	5.25 (0.28)
5		>50 (<0.22)	>50 (<0.22)
6	H	>50 (<0.28)	>50 (<0.28)
7		0.6 (0.32)	1.1 (0.30)

^a IC_{50} values are given in μM .

Scheme 1. Three-Step Synthesis of Imidazole Small Molecule Ligand^a



^aReagents and conditions. Van Leusen Reaction: Aldehyde (1.0 equiv), amine (1.5 equiv), glacial acetic acid (2.0 equiv), ethanol, reflux, 4 h; then evaporation, K_2CO_3 (2.0 equiv), TosMIC (1.5 equiv), DMF, 95 °C. Bromination: DBDMH (0.5 equiv), DMF, 0–25 °C, 20 h. C–C Bond Formation: $Pd(PPh_3)_4$ (0.08 equiv), Stille reagent (2.0 equiv), dioxane, 150 °C under microwaves, 1.5 h.

66% yield. Regioselective bromination of imidazole (35–67% yield) and microwave assisted Stille (45–54% yield) or Suzuki (6–47% yield) coupling gave the final compounds **1**, **2**, **3**, **4**, and **7**. For the synthesis of **5**, we used a two-step process from the brominated imidazole involving a palladium catalyzed formation of the corresponding alkyne followed by a 1,3-dipolar cycloaddition with chloro acetaldoxime (30% yield over two steps).

We initially tested all compounds using AlphaScreen assays.¹⁷ The pyridine **2** showed a significant improvement in activity, suggesting that the pyridine nitrogen indeed engaged in a hydrogen bond with one of the conserved water molecules at the base of the pocket. Interestingly, the meta pyridine **3** was inactive, very likely because the pyridine nitrogen is situated in a less favorable position to interact with the water molecules compared to **2**. The thiazole **4** demonstrated that 5-membered KAc mimetics can also exhibit improved activity. Finally, we prepared and tested **5** and **7**, both featuring 5-membered KAc mimetics that we designed to engage in a hydrogen bond and mimic the terminal methyl group of KAc through a methyl substituent. Interestingly, these gave very different results. Isoxazole **5** did not inhibit BAZ2A and B to a significant degree, which was surprising given that the methyl isoxazole is a well-known KAc mimetic (vide infra). The pyrazole derivative **7**, on the other hand, was the most potent inhibitor out of this initial set with IC_{50} values of 0.6 and 1.07 μM for BAZ2A and BAZ2B, respectively. We had thus achieved an almost 100-fold increase in potency for BAZ2A and a 25-fold increase for BAZ2B without increasing molecular weight, thus also improving the ligand efficiency (Table 1).

To support our design hypothesis, we subsequently determined the crystal structure (2.0 Å) of BAZ2B in complex with **7** to confirm the acetyl-lysine mimetic binding mode of the introduced methyl pyrazole (Figure 2). The pyrazole acted indeed as an acetyl-lysine mimetic moiety, forming a hydrogen bond with a conserved water molecule that also interacts with the conserved Y1901. Superimposition of **7**- and KAc-complexed structures¹² confirmed that the methyl substituent of pyrazole occupied the position typically filled by the terminal methyl group of KAc. In all other aspects, the cocrystal structure of **7** resembled the structure of **1** bound to BAZ2B, confirming that the increased activity in **7** was indeed due to the optimized KAc mimetic.¹⁸ To our knowledge, this represented the first example of a pyrazole moiety as the KAc mimetic in a bromodomain inhibitor.

The insights from the crystal structure of **7** also provided a potential explanation why **5**, which featured a methyl

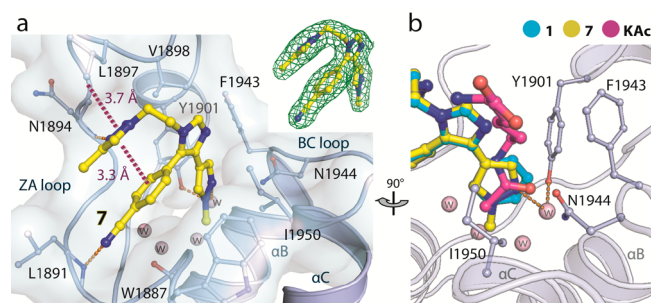


Figure 2. Crystal structure of the BAZ2B bromodomain in complex with **7**. (a) Detailed interaction between **7** (yellow stick) and BAZ2B in the crystal structure with $|2F_o| - |F_c|$ omitted map contoured at 1 σ for **7** shown in the inset (PDB: 4XUB). Hydrogen bonds are shown as dashed orange lines, while the dashed magenta lines indicated the smallest distances between the triazole ring to the π -stacking partner benzonitrile and to L1897. (b) Superimposition of the BAZ2B–**1**, –**7**, and –KAc complexes. Conserved water molecules bound within the KAc binding site are shown in pink spheres.

substituted isoxazole (a well-known BET bromodomain inhibitor warhead), was completely inactive. The oxygen atom cannot engage in hydrogen bond to the conserved asparagine as it does in complexes with other bromodomains.³ The increased desolvation penalty caused by the additional acceptor is thus not compensated through a hydrogen bond. Furthermore, we speculated that differences in the conformational preferences of the pyrazole and the isoxazole ring contributed to the lack of activity. We performed an analysis of the preferred torsion angles between the imidazole on one hand and the pyrazole ring of **7** and the isoxazole ring of **5** on the other hand, while the rest of the molecules was kept in the bioactive conformation. In the case of **7**, the torsion angle with the lowest predicted energy is indeed similar to the torsion angle observed in the crystal structure. In strong contrast, our analysis of **5** predicted a lowest energy torsion angle that is not compatible with binding because the isoxazole methyl group pointed in the opposite direction compared to the pyrazole methyl substituent of **7** (see SI). This conformation is likely preferred because it allowed a more coplanar orientation of the isoxazole with the imidazole (10° deviation from the coplanar orientation compared to 30° for the conformation compatible with binding). Penalties due to desolvation and higher energy conformation thus collectively cause the complete loss of activity for **5**.

Having achieved a large leap in activity, we decided to investigate whether **7** adopts the stacked, bioactive conformation evident from crystal structure upon binding to the target or whether this bioactive conformation is already populated to a significant degree in solution prior to binding to BAZ2A/B. We hypothesized that if the former was the case, binding to BAZ2 will result in a free energy penalty caused by adopting the bioactive conformation. In this scenario, stabilizing this conformation might reduce the penalty and result in an increase in activity.

To investigate the solution conformation of **7**, we used ¹H NMR spectroscopy.

We hypothesized that in the stacked conformation the signals of protons H-2'/H-6' (Figure 3, labeled in red) will shift significantly upfield due to the anisotropic effect arising from the ring current of triazole ring compared to **8**, which does not feature the triazole ring.¹⁹ However, the H-2'/H2-6' protons of **7** and **8** showed near identical chemical shifts in D₂O.

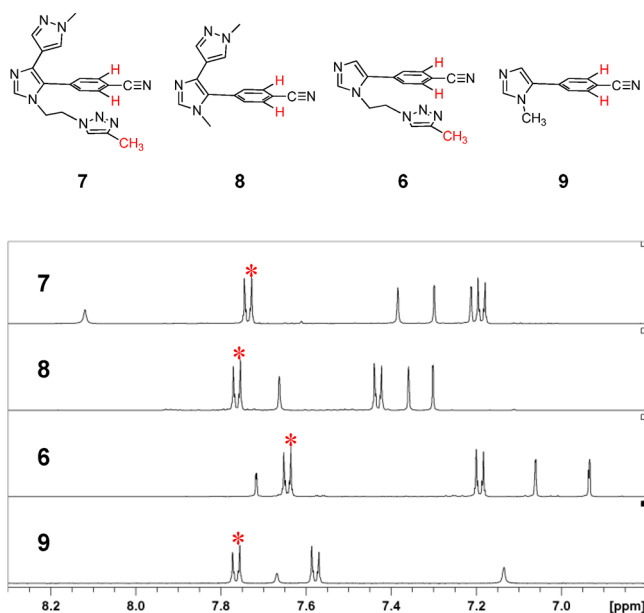


Figure 3. Conformations of **6**, **7**, **8**, and **9** were investigated by ^1H NMR in D_2O at 295 K. The red asterisks mark the signals from protons ortho to the nitrile group.

Furthermore, the ^1H – ^1H NOESY spectrum of **7** did not show a correlation between these protons and the protons on the methyl group of the triazole ring (see SI). Both results suggested that **7** did not adopt the π -stacking conformation to a significant degree in solution.

Interestingly, when we performed a similar set of experiments for intermediate **6** (Figure 3), a clear shift of the protons (0.12 ppm) compared to **9** as well as a NOESY correlation were apparent, strongly indicating that contrary to **7** the less substituted **6** does adopt a conformation in solution in which the two aryl rings are in close proximity. While **6** did not show significant binding (Table 1), this validated the NMR method, thus further increasing our confidence that **7** did not adopt the bioactive conformation to a large degree in solution. The different behavior with regard to the conformation in solution between **6** and **7** is likely caused by the additional heteroaryl substituent of **7** that makes adoption of this conformation less favorable.

On the basis of the crystal structure of **7** and the observation that **7** did not adopt the bioactive conformation in solution, we next designed a set of follow up compounds to further increase the potency by optimizing the interactions with the protein and stabilizing the bioactive, stacked conformation (Table 2).

Compounds **10**, **11**, and **12** feature electron withdrawing fluorine or nitro substituents at the phenyl ring to increase the electron withdrawing character of the phenyl ring and strengthen the electronic component of the stacking interaction. Our modeling experiments suggested that the nitro group of **12** was well placed to engage in the same hydrogen bonding interaction with the backbone donor of Leu1891 as the nitrile group in **7**.

Furthermore, inspection of the crystal structure revealed that N2 of the triazole ring was situated in a hydrophobic environment formed by the side chains of Leu1897, Val1893, and Val1898 and did not engage in a hydrogen bond. We hypothesized that removing this nitrogen atom reduces the desolvation penalty, increases the hydrophobic interactions with the protein, and increases the electron rich character of

Table 2. Structure–Activity Relationship of *N*-Methyl Pyrazole Substituted Compounds^a

			BAZ2A	BAZ2B
	R1	R2	IC ₅₀ (LE)	IC ₅₀ (LE)
7			0.6 (0.32)	1.07 (0.30)
8		H	>50 (<0.29)	>50 (<0.29)
10			1.01 (0.29)	0.77 (0.30)
11			0.45 (0.31)	0.79 (0.30)
12			1.38 (0.29)	2.45 (0.28)
13 (BAZ2-ICR)			0.13 (0.35)	0.18 (0.34)

^aIC₅₀ values are given in μM .

this ring and thus the stability of the stacked conformation. This led us to **13**.

To investigate the importance of these groups, along with **10**–**13**, we prepared **8** in which the entire triazole group is removed. The screening results for this second set of compounds are summarized in Table 2.

The complete loss of activity of **8**, in which one-half of the internal π -stacking has been removed, reinforces the importance of this element for potent binding. As can be further seen from Table 2, addition of a fluorine atom at both positions of the phenyl ring was largely tolerated for BAZ2A and BAZ2B but did not lead to a significant increase in activity. The same held true for the nitro compound **12** that showed comparable activity to **7**.

Gratifyingly, replacement of the triazole with the pyrazole led to a 5-fold increase in activity. Compound **13** inhibits BAZ2A and BAZ2B with IC₅₀s of 130 and 180 nM, respectively, thus reaching our targeted potency. Compared to our starting point **1**, **13** possesses a 200-fold increase in activity.

We performed the NMR experiments described above with **13**. However, as for **7**, the absence of a chemical shift and a correlation of the protons in question in the ^1H – ^1H NOESY spectrum strongly indicated that **13** did not adopt the bioactive

conformation to significant degree in solution. On the basis of this observation, we believed that the increased potency was indeed caused by improved hydrophobic interactions and decreased desolvation penalty upon binding.

Next, we investigated the binding of **13** to BAZ2A/B by isothermal titration calorimetry (ITC).

In very good agreement with the IC_{50} s, the compound showed K_d s of 109 and 170 nM to BAZ2A and BAZ2B, respectively (Figure 4). Interestingly, the binding was driven by

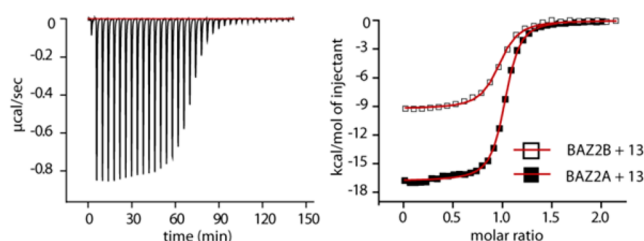


Figure 4. ITC data of the interaction of **13** with BAZ2A and BAZ2B. Raw BAZ2A binding heats are shown in the left panel as well as normalized integrated binding enthalpies for each injection in the right panel. Nonlinear least-squares fits are shown as red solid lines.

large enthalpic contributions ($\Delta H = 17$ kcal/mol for BAZ2A and 9 kcal/mol for BAZ2B) and a loss of entropy, which is consistent with a loss of conformational freedom of **13** due to adoption of the bioactive conformation upon binding.

Having achieved our targeted potency, we next assessed the selectivity of **13** by screening the compound against 47 bromodomains using thermal shift (Figure 5).²⁰ The data are visualized in Figure 5, and numerical values as well as available control compounds are compiled in the SI.

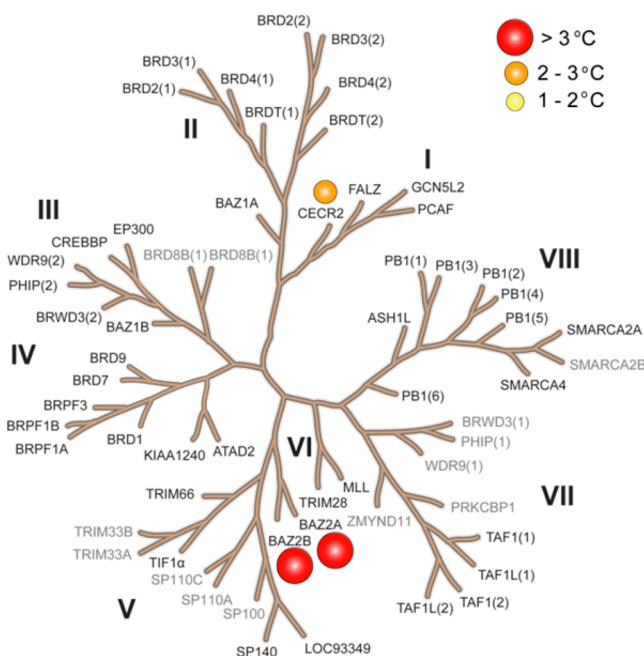


Figure 5. Selectivity of **13**. The inhibitor was screened at 10 μ M concentration against 47 bromodomains using temperature shift assay. The screened targets are labeled on the phylogenetic tree, whereas targets that have not been screened are shown in gray. Temperature shifts are represented as spheres as indicated in the figure.

In agreement with the potent binding shown in our biochemical assays as well as ITC, **13** showed significant thermal shifts of 5.2 and 3.8 $^{\circ}$ C for BAZ2A and BAZ2B respectively. Gratifyingly, **13** did not show significant thermal shifts against all other bromodomains, except for Cat Eye syndrome chromosome region, candidate 2 (CECR2), where we observed a smaller but significant shift (ΔT_m : 2.0 $^{\circ}$ C). We determined the K_d of **13** to CECR2 by ITC to be 1.55 μ M, therefore resulting in a 15-fold selectivity when compared to BAZ2A and a 10-fold window to BAZ2B.

To ensure that our probe showed a sufficient window to the BET bromodomains, we tested **13** in a BRD4 AlphaScreen assay, where it did not show significant inhibition up to 50 μ M translating in greater than 100-fold window. Furthermore, we confirmed the selectivity against BRD4 in a cellular assay (vide infra). Molecule **13** thus overall shows a very high degree of selectivity within the bromodomain family.

Furthermore, a receptor screening performed at CEREP against 55 possible off-targets returned a very clean profile (see SI).

To investigate whether **13** can displace BAZ2 bromodomains from chromatin in living cells, we performed a fluorescence recovery after photobleaching (FRAP) assay utilizing GFP-tagged BAZ2A full length protein transfected into human osteosarcoma cells (U2OS). As a control we used a mutant (N1873F) that does not bind KAc containing peptides and therefore mirrors the behavior of inhibitor bound BAZ2A. In addition, we used the histone deacetylase (HDAC) inhibitor SAHA to increase overall levels of histone acetylation, resulting in a sufficient window measuring differences in recovery time and demonstrating the acetylation dependence of the FRAP experiments (Figure 6). Importantly, 1 μ M **13** reduced the recovery time of the wild-type (wt) construct to a level similar to the dominant negative mutant, confirming that **13** inhibits BAZ2A in cells.

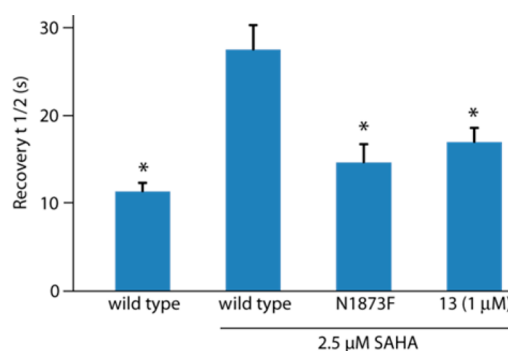


Figure 6. Fluorescence recovery after photobleaching (FRAP) assay data. Shown are recovery half times of wild-type and SAHA treated cells as well as the bromodomain inactivating mutant (N1873F) and **13** treated wild-type cells. * $P < 0.05$, significant difference from wt treated with SAHA.

To confirm selectivity in the cellular setting, we performed a similar FRAP assay for BRD4 where **13** did not show any significant activity (see SI).

Ideally, chemical probes can be used in vitro as well as in vivo. To investigate whether **13** is suitable for in vivo experiments, we assessed its physicochemical and mouse pharmacokinetic properties. Compound **13** showed very high solubility (25 mM in D₂O), a measured log D of 1.05, high stability in mouse microsomes, and permeation in the CaCo-2

model (see SI) and thus a suitable profile for oral and intravenous gavage. We therefore performed a full mouse pharmacokinetic experiment. In agreement with the in vitro data, **13** showed 70% bioavailability and moderate clearance (~50% of mouse liver blood flow) and volume of distribution (see SI). This set of data therefore suggested that **13** is suitable for modulating BAZ2A and BAZ2B in vivo.

CONCLUSIONS

We describe the discovery of a potent and selective chemical probe to target BAZ2A and BAZ2B bromodomains starting from a weakly potent hit. We achieved a greater than 100-fold improvement in potency in just two cycles of design and synthesis, underscoring the power of structure based design.

Moreover, our work highlights the utility of intramolecular π -stacking to target challenging binding sites. In strong contrast to many other bromodomains, e.g., the BET subfamily, BAZ2A and B, show a low degree of druggability due to an open binding pocket that lacks the high degree of enclosure observed for BRD4. Recently, the concept of molecules featuring a three-dimensional shape has been proposed to target open pockets, e.g., in the context of protein–protein interactions.²¹ In particular, intramolecular π -stacking arrangements represent an unusual example of this concept in that they consist of two flat components that reversibly associate to form a three-dimensional shape. Our inhibitors exemplify that π -stacking arrangements can effectively provide shape complementarity and extensive hydrophobic and polar contacts for open, less enclosed pockets. Interestingly, a π -stacking arrangement has been observed for inhibitors of BCL2, another protein–protein interaction target.²²

Because of its excellent in vitro and in vivo profile, **13** (BAZ2-ICR) satisfies the criteria for a dual BAZ2A and BAZ2B chemical probe. The compound is freely available to the scientific community via <http://www.thesgc.org/chemical-probe/BAZ2-ICR>. Experiments to investigate biological role of BAZ2A and B are underway and will be published in due course.

ASSOCIATED CONTENT

Supporting Information

Experimental and characterization details for all new compounds, computational data, ITC data, assays data, crystallographic data, pharmacokinetic data, and NMR spectra. This material is available free of charge via the Internet at <http://pubs.acs.org>.

AUTHOR INFORMATION

Corresponding Authors

*For S.H.: phone, +44 2087224353; E-mail, swen.hoelder@icr.ac.uk.

*For S.K. phone, +44 1865612933; E-mail, stefan.knapp@sgc.ox.ac.uk.

Notes

The authors declare no competing financial interest.

ACKNOWLEDGMENTS

Lewis Vidler was funded by Cancer Research UK (grant no. C309/A11369), Sally McGrath was funded by Wellcome Trust (grant no. 090171/Z/09/Z), Wasim Akhtar was funded by EPSRC DTG (grant no. EP/J500240/1). We acknowledge NHS funding to the NIHR Biomedical Research Centre and

funding from Cancer Research UK (grant no. C309/A11566). The SGC is a registered charity (no. 1097737) that receives funds from AbbVie, Bayer Pharma AG, Boehringer Ingelheim, the Canada Foundation for Innovation, Genome Canada, GlaxoSmithKline, Janssen, Lilly Canada, the Novartis Research Foundation, the Ontario Ministry of Economic Development and Innovation, Pfizer, Takeda, and the Wellcome Trust (092809/Z/10/Z).

REFERENCES

- (1) Filippakopoulos, P.; Knapp, S. Targeting Bromodomains: Epigenetic Readers of Lysine Acetylation. *Nature Rev. Drug Discovery* **2014**, *13*, 337–356.
- (2) Muller, S.; Filippakopoulos, P.; Knapp, S. Bromodomains as Therapeutic Targets. *Expert Rev. Mol. Med.* **2011**, *13*, e29.
- (3) Hay, D. A.; Fedorov, O.; Martin, S.; Singleton, D. C.; Tallant, C.; Wells, C.; Picaud, S.; Philpott, M.; Monteiro, O. P.; Rogers, C. M.; Conway, S. J.; Rooney, T. P.; Tumber, A.; Yapp, C.; Filippakopoulos, P.; Bunnage, M. E.; Muller, S.; Knapp, S.; Schofield, C. J.; Brennan, P. E. Discovery and Optimization of Small Molecule Ligands for the CBP/p300 Bromodomains. *J. Am. Chem. Soc.* **2014**, *136*, 9308–9319.
- (4) Weiss, W. A.; Taylor, S. S.; Shokat, K. M. Recognizing and Exploiting Differences Between RNAi and Small-Molecule Inhibitors. *Nature Chem. Biol.* **2007**, *3*, 739–744.
- (5) Jones, M. H.; Hamana, N.; Nezu, J.; Shimane, M. A Novel Family of Bromodomain Genes. *Genomics* **2000**, *63*, 40–45.
- (6) Strohnner, R.; Nemeth, A.; Jansa, P.; Hofmann-Rohrer, U.; Santoro, R.; Langst, G.; Grummt, I. NoRC—A Novel Member of Mammalian ISWI-Containing Chromatin Remodeling Machines. *EMBO J.* **2001**, *20*, 4892–4900.
- (7) Mayer, C.; Neubert, M.; Grummt, I. The Structure of NoRC-Associated RNA is Crucial for Targeting the Chromatin Remodelling Complex NoRC to the Nucleus. *EMBO Rep.* **2008**, *9*, 774–780.
- (8) Zhou, Y.; Grummt, I. The PHD Finger/Bromodomain of NoRC Interacts with Acetylated Histone H4K16 and is Sufficient for rDNA Silencing. *Curr. Biol.* **2005**, *15*, 1434–1438.
- (9) Arking, D. E.; Junttila, M. J.; Goyette, P.; Huertas-Vazquez, A.; Eijgelsheim, M.; Blom, M. T.; Newton-Cheh, C.; Reinier, K.; Teodorescu, C.; Uy-Evanado, A.; Carter-Monroe, N.; Kaikkonen, K. S.; Kortelainen, M. L.; Boucher, G.; Lagace, C.; Moes, A.; Zhao, X.; Kolodgie, F.; Rivadeneira, F.; Hofman, A.; Witteman, J. C.; Uitterlinden, A. G.; Marsman, R. F.; Pazoki, R.; Bardai, A.; Koster, R. W.; Dehghan, A.; Hwang, S. J.; Bhatnagar, P.; Post, W.; Hilton, G.; Prineas, R. J.; Li, M.; Kottgen, A.; Ehret, G.; Boerwinkle, E.; Coresh, J.; Kao, W. H.; Psaty, B. M.; Tomaselli, G. F.; Sotoodehnia, N.; Siscovick, D. S.; Burke, G. L.; Marban, E.; Spooner, P. M.; Cupples, L. A.; Jui, J.; Gunson, K.; Kesaniemi, Y. A.; Wilde, A. A.; Tardif, J. C.; O'Donnell, C. J.; Bezzina, C. R.; Virmani, R.; Stricker, B. H.; Tan, H. L.; Albert, C. M.; Chakravarti, A.; Rioux, J. D.; Huikuri, H. V.; Chugh, S. S. Identification of a Sudden Cardiac Death Susceptibility Locus at 2q24.2 Through Genome-Wide Association in European Ancestry Individuals. *PLoS Genet.* **2011**, *7*, e1002158.
- (10) Gu, L.; Frommel, S. C.; Oakes, C. C.; Simon, R.; Grupp, K.; Gerig, C. Y.; Bär, D.; Robinson, M. D.; Baer, C.; Weiss, M.; Gu, Z.; Schapira, M.; Kuner, R.; Sülthmann, H.; Provenzano, M.; ICGC Project on Early Onset Prostate Cancer, Yaspo, M.-L.; Brors, B.; Korb, J.; Schlomm, T.; Sauter, G.; Eils, R.; Plass, C.; Santoro, R. BAZ2A (TIP5) is Involved in Epigenetic Alterations in Prostate Cancer and its Overexpression Predicts Disease Recurrence. *Nature Genet.* **2014**, DOI: 10.1038/ng.3165.
- (11) Vidler, L. R.; Brown, N.; Knapp, S.; Hoelder, S. Druggability Analysis and Structural Classification of Bromodomain Acetyl-Lysine Binding Sites. *J. Med. Chem.* **2012**, *55*, 7346–7359.
- (12) Ferguson, F. M.; Fedorov, O.; Chaikuad, A.; Philpott, M.; Muniz, J. R.; Felletar, I.; von Delft, F.; Heightman, T.; Knapp, S.; Abell, C.; Ciulli, A. Targeting Low-Druggability Bromodomains: Fragment Based Screening and Inhibitor Design Against the BAZ2B Bromodomain. *J. Med. Chem.* **2013**, *56*, 10183–10187.

- (13) Vidler, L. R.; Filippakopoulos, P.; Federov, O.; Picaud, S.; Martin, M.; Tomsett, M.; Woodward, H.; Brown, N.; Knapp, S.; Hoelder, S. Discovery of Novel Small-Molecule Inhibitors of BRD4 Using Structure-Based Virtual Screening. *J. Med. Chem.* **2013**, *56*, 8073–8088.
- (14) (a) Filippakopoulos, P.; Knapp, S. The Bromodomain Interaction Module. *FEBS Lett.* **2012**, *586*, 2692–2704. (b) Filippakopoulos, P.; Picaud, S.; Mangos, M.; Keates, T.; Lambert, J. P.; Barsyte-Lovejoy, D.; Felletar, I.; Volkmer, R.; Muller, S.; Pawson, T.; Gingras, A. C.; Arrowsmith, C. H.; Knapp, S. Histone Recognition and Large-Scale Structural Analysis of the Human Bromodomain Family. *Cell* **2012**, *149*, 214–231.
- (15) Salonen, L. M.; Ellermann, M.; Diederich, F. Aromatic Rings in Chemical and Biological Recognition: Energetics and Structures. *Angew. Chem., Int. Ed.* **2011**, *50*, 4808–4842.
- (16) Cheeseright, T. J.; Mackey, M. D.; Scoffin, R. A. High Content Pharmacophores from Molecular Fields: A Biologically Relevant Method for Comparing and Understanding Ligands. *Curr. Comput.-Aided Drug Des.* **2011**, *7*, 190–205.
- (17) Philpott, M.; Yang, J.; Tumber, T.; Fedorov, O.; Uttarkar, S.; Filippakopoulos, P.; Picaud, S.; Keates, T.; Felletar, I.; Ciulli, A.; Knapp, S.; Heightman, T. D. Bromodomain-Peptide Displacement Assays for Interactome Mapping and Inhibitor Discovery. *Mol. Biosyst.* **2011**, *7*, 2899–2908.
- (18) Sharp, P. P.; Garnier, J.-M.; Huang, D. C. S.; Burns, C. J. Evaluation of Functional Groups as Acetyl-Lysine Mimetics for BET Bromodomain Inhibition. *Med. Chem. Commun.* **2014**, *5*, 1834–1842.
- (19) Nandy, R.; Subramoni, M.; Varghese, B.; Sankararaman, S. Intermolecular π -Stacking Interaction in a Rigid Molecular Hinge Substituted with 1-(Pyrenylethynyl) Units. *J. Org. Chem.* **2007**, *72*, 938–944.
- (20) Filippakopoulos, P.; Qi, J.; Picaud, S.; Shen, Y.; Smith, W. B.; Fedorov, O.; Morse, E. M.; Keates, T.; Hickman, T. T.; Felletar, I.; Philpott, M.; Munro, S.; McKeown, M. R.; Wang, Y.; Christie, A. L.; West, N.; Cameron, M. J.; Schwartz, B.; Heightman, T. D.; La Thangue, N.; French, C. A.; Wiest, O.; Kung, A. L.; Knapp, S.; Bradner, J. E. Selective Inhibition of BET Bromodomains. *Nature* **2010**, *468*, 1067–1073.
- (21) Morley, A. D.; Pugliese, A.; Birchall, K.; Bower, J.; Brennan, P.; Brown, N.; Chapman, T.; Drysdale, M.; Gilbert, I. H.; Hoelder, S.; Jordan, A.; Ley, S. V.; Merritt, A.; Miller, D.; Swarbrick, M. E.; Wyatt, P. G. Fragment-Based Hit Identification: Thinking in 3D. *Drug Discovery Today* **2013**, *18*, 1221–1227.
- (22) Oltersdorf, T.; Elmore, S. W.; Shoemaker, A. R.; Armstrong, R. C.; Augeri, D. J.; Belli, B. A.; Bruncko, M.; Deckwerth, T. L.; Dinges, J.; Hajduk, P. J.; Joseph, M. K.; Kitada, S.; Korsmeyer, S. J.; Kunzer, A. R.; Letai, A.; Li, C.; Mitten, M. J.; Nettesheim, D. G.; Ng, S.; Nimmer, P. M.; O'Connor, J. M.; Oleksijew, A.; Petros, A. M.; Reed, J. C.; Shen, W.; Tahir, S. K.; Thompson, C. B.; Tomaselli, K. J.; Wang, B.; Wendt, M. D.; Zhang, H.; Fesik, S. W.; Rosenberg, S. H. An Inhibitor of Bcl-2 Family Proteins Induces Regression of Solid Tumours. *Nature* **2005**, *435*, 677–681.